Available online at www.sciencedirect.com
ScienceDirect
Journal of Solid State Chemistry 181 (2008) 130–136
JOURNAL OF SOLID STATE CHEMISTRY
www.elsevier.com/locate/jssc

Synthesis and characterization of substitutional and interstitial nitrogen-doped titanium dioxides with visible light photocatalytic activity

Feng Peng*, Lingfeng Cai, Hao Yu, Hongjuan Wang, Jian Yang

School of Chemical and Energy Engineering, South China University of Technology, Guangzhou 510640, PR China

Received 19 July 2007; received in revised form 4 November 2007; accepted 12 November 2007
Available online 19 November 2007

Abstract

Both substitutional and interstitial nitrogen-doped titanium dioxides (N-TiO_2) were prepared. Their surface states were clarified by XPS spectra of N 1*s*, O 1*s* and Ti 2*p*. The results of photocatalysis show that both substitutional and interstitial N impurities greatly enhance the photoactivity of TiO_2 in visible light. Moreover, the visible light activity of interstitial N-doped TiO_2 is higher than that of substitutional N-doped TiO_2. The microwave synthesis presented in this paper is a promising and practical method to produce interstitial nitrogen-doped photocatalysts with high visible light activity.

Keywords: Nitrogen-doped titania; Surface structure; Microwave synthesis; Photocatalysis; X-ray photoelectron spectroscopy

1. Introduction

A number of developments on visible light sensitive TiO_2 have been made about how to efficiently utilize the solar energy or rays from artificial sources in photocatalytic reactions [1–7]. Asahi et al. demonstrated $TiO_{2-x}N_x$ films prepared by sputtering TiO_2 target in a mixture of N_2/Ar gas showed higher photocatalytic reactivity under visible light irradiation compared to conventional TiO_2 thin films [8]. From then on, doping with nitrogen has been considered one of most effective approaches to improve photocatalytic activity of TiO_2 in visible region [9–15]. Recently, many groups reported visible light photocatalysis of N-doped TiO_2 prepared by different methods [16–26], such as ion implantation [16], sputtering [17,18], chemical vapor deposition [19–22], sol–gel [12,23], and decomposition of N-containing metal organic precursors [24].

Hitherto, studies about the effect of preparation methods on the chemical nature and photoactivity of N-doped TiO_2 under visible light irradiation are relatively few. The photocatalysis mechanism of TiO_2 in visible light is very confused. Most of reports agreed on that N 1*s* peak at 396–398 eV is characteristic peak of Ti–N–Ti linkages, indicating nitrogen atom is doped into the TiO_2 lattice [27–30] and responsible for enhanced activity. However, N 1*s* peak around 396 eV was not always observed. Different N 1*s* peaks at 400–404 eV have also been reported and correlated with the photoactivity in visible light [28,31]. In this paper, we prepared two types of N-TiO_2, and used them to decompose methyl orange dye and phenol under visible light radiation. We clarified the effect of preparation methods on the formation mechanism of N-TiO_2, and the effect of types of nitrogen-doping in TiO_2 on photocatalytic activity in visible light.

2. Experimental

In a typical experiment, 0.8 g of P25 (Degussa) TiO_2 powder and 1.2 g of urea were mixed with 40 ml ethylene glycol. To disperse them homogeneously, the mixture was exposed to high-intensity ultrasound irradiation for 15 min. The suspension was transferred to a telfon cup that then was placed into a multi-mode microwave oven (MAS-II, Shanghai Sineo Microwave Chemistry Technology Co. Ltd.) operated at 1000 W and 2450 MHz for 10–30 min.

*Corresponding author. Fax: +86 20 87113735.
E-mail address: cefpeng@scut.edu.cn (F. Peng).

0022-4596/$ - see front matter © 2007 Elsevier Inc. All rights reserved.
doi:10.1016/j.jssc.2007.11.012

The temperature was set above 135 °C, higher than the decomposition temperature of urea. After the suspension was cooled down to room temperature, the precipitate was centrifuged, washed by deionized water and absolute ethanol for several times, and dried at 100 °C in air for 10 h. As-synthesized yellowish powder of nitrogen-doped titanium dioxide was denoted as N-TiO_2-M. This sample was further treated at 300 °C in air for 2 h, which was labeled as N-TiO_2-M-300. For comparison, 0.5 g of P25–TiO_2 powder was annealed under NH_3 flow at 600 °C for 3 h as a reference sample [8,21], which was denoted as N-TiO_2-NH_3.

The crystal structure of samples was characterized by powder XRD on a X-ray diffractometer (D/max-IIIA, Japan) using Cu *Kα* radiation and operating at 30 kV/30 mA in the angle range of 5–70°. The chemical nature of N in TiO_2 was studied using XPS by a Krato Axis Ultra DLD spectrometer with Al *Kα* X-ray ($h\nu = 1486.6$ ev) at 15 kV and 150 W. The binding energy was referenced to C 1*s* line at 284.9 eV for calibration. Infrared spectroscopy (Bruker 550) was used to identify the surface organic groups in different TiO_2 and study their influence on the nitridation process. The UV–vis light absorption spectra were obtained from a Hitachi UV-3010 spectrophotometer equipped with an integrating sphere assembly, using the diffuse reflection method and $BaSO_4$ as a reference to measure all the samples.

The photocatalytic reaction was conducted in a 200 ml cylindrical glass vessel fixed in a XPA-II photochemical reactor (Nanjing Xujiang Machine-electronic Plant). The reactor consists of several components, such as light source system, filter system, magnetic stirrer and quartz cool trap that can lower the reaction temperature and prevent the evaporation of water. One thousand watt Xe lamp was used as simulated solar light source, due to similar spectral features to solar light. The filter system comprises a house-made filter mounted on the lamp to eliminate infrared irradiation and a UV filter made from 1 M sodium nitrate solution that can absorb the light with wavelength less than 400 nm [32]. The variation of solutions used as the filter could effective changes wavelength of irradiation light on catalysts. Methyl orange dye (MO) was used as reactant with the concentration of 20 mg/l. In order to avoid the influence of dye-sensitized mechanism on photocatalysis results, phenol was also used as a model to study the degradation of organic pollutants in visible light. Photocatalyst powder of 40 mg was dispersed in 200 ml solutions with the concentration of phenol at 100 mg/l. The solution was sonicated for 15 min to obtain an optimally dispersed system and then put in a black box for 60 min to reach complete adsorption/desorption equilibrium. Further details of photocatalytic reaction and analysis method could be found in Ref. [33]. The concentrations of remaining MO or phenol were surveillanced by measuring its absorbance (A) at 465 or 269.5 nm, respectively, with a Hitachi UV-3010 spectrophotometer. The degradation ratio (X) of reactant can be calculated by $X(\%) = 100(A_0 - A)/A_0$.

3. Results and discussion

The XRD patterns of different TiO_2 samples are shown in Fig. 1. The presence of mixed phases of anatase and rutile is observed for all samples. However, no N-derived peak is detected for N-TiO_2. Thus, N doping does not cause the change in crystallite structure of TiO_2, which is consistent with Refs. [27,34]. The anatase crystal sizes of samples were calculated using the Scherrer equation. The calculation results of different samples are given in Table 1. It can be seen from Table 1 that there is no obvious change in phase component for N-TiO_2-M and N-TiO_2-NH_3 after the microwave reaction and calcination. BET specific surface areas of N-TiO_2-M and N-TiO_2-NH_3 are decreased slightly compared with P25–TiO_2 powder. From the above analyses, it is revealed that the microstructures of the TiO_2 could be preserved after different treatments.

The XPS spectra of P25 and nitrogen-doped TiO_2 samples are shown in Fig. 2. The surfaces of the TiO_2 samples are composed of Ti, O and carbon contaminant. There are obvious nitrogen signals in the N-doped samples, although peak intensities are not so strong. Fig. 2(b) clearly shows the binding energies of N 1*s* at 396.5 and 399.9 eV for N-TiO_2-NH_3 and N-TiO_2-M, respectively. Asahi et al. [8] assigned the atomic β-N (396 eV) peak to substitutional N, which may be related to the active sites in photocatalysis. Most researchers also agree on N 1*s* peak at

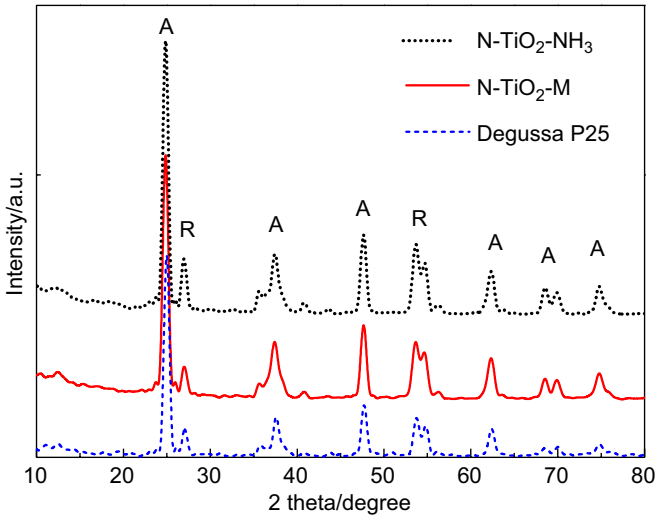

Fig. 1. XRD patterns of different TiO_2 samples.

Table 1
Analysis of crystal phases and BET specific surface area for different samples

Sample	Anatase crystal size (nm)	Anatase fraction (%)	Rutile fraction (%)	BET (m^2/g)
P25	26.2	87.7	12.3	50.5
N-TiO_2-NH_3	25.2	87.3	12.7	46.1
N-TiO_2-M	22.5	84.1	15.9	46.9

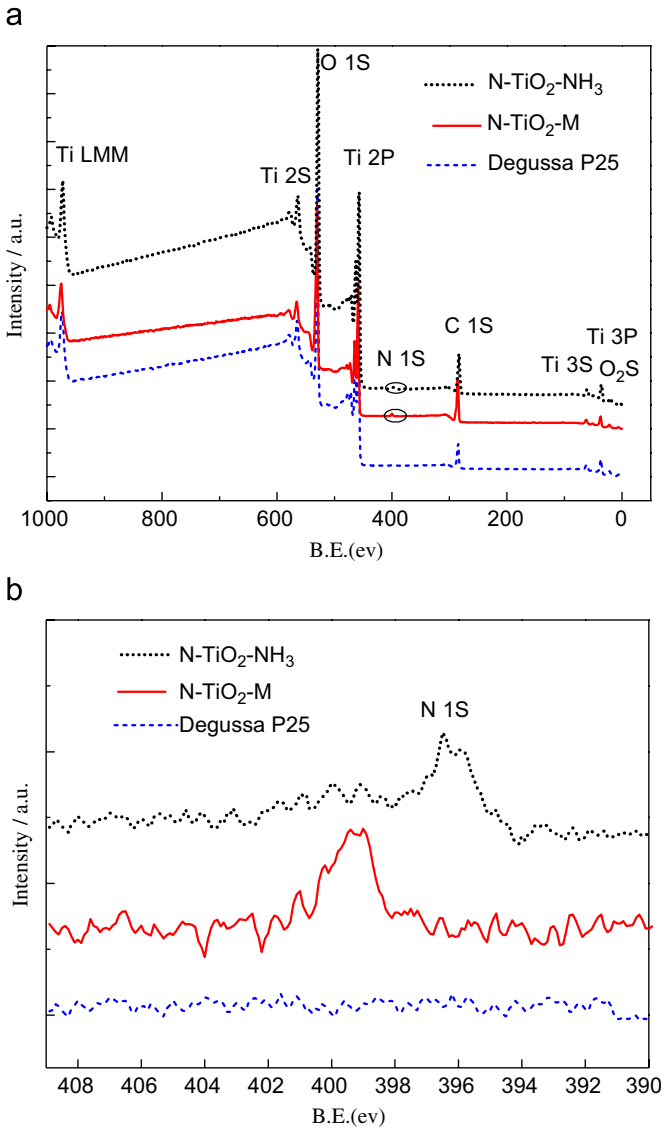

Fig. 2. Survey (a) and N 1*s* (b) XPS spectra of TiO_2, N-TiO_2-M and N-TiO_2-NH_3.

396–397.5 eV responsible for nitrogen atoms substitutionally doped into the TiO_2 lattice as characteristic peak of Ti–N–Ti linkages [27–30]. Therefore, N 1*s* peak at 396.5 eV can be attributed to Ti–N–Ti linkages in N-TiO_2 (N 1*s* peak at 397.5 eV for TiN [27,30]), resulting from the nitrogen substitution of oxygen in the TiO_2 lattice. Although the N 1*s* peak at around 400 eV has been reported, no consensus has been achieved about its nature [8,21–24,27]. It has been reported that N 1*s* peak at around 400 eV can be assigned to molecularly chemisorbed γ-N [35]. Some researches suggested that N 1*s* peak at 399–400 eV is due to NH_3 adsorbed on the surface [8,31]. In the absent of NH_3 adsorbed on the surface, however, the N 1*s* peak at around 400 eV has also been observed. Because the N 1*s* BE is higher with the more positive formal charge (e.g., 408 eV in $NaNO_3$) compared with zero or a negative formal charge (398.8 eV in NH_3) [10,28], many researches pointed out the presence of oxidized nitrogen such as Ti–O–N and/or Ti–N–O linkages should appear above 400 eV [27–30]. Di Valentin et al. [36] have reported that a significant advance toward the clarification of the above issues by means of electron paramagnetic resonance spectroscopy measurements and DFT calculations. They presented there were two types of N species in N-TiO_2; their spin-Hamiltonian parameters were consistent with calculations for both substitutional and interstitial N impurities. Although not proven experimentally, it was inferred from theory [37]. We attributed N 1*s* peak at 400 eV to a characteristic peak of interstitial N, namely hosted in an interstitial position and directly bound to lattice oxygen, for N-TiO_2-M prepared by microwave method. The interstitial N is in a positive oxidation state ranged from that of typical hyponitrite species $(N_2O_2)^{2-}$ to nitrite (NO_2^-) and nitrate species (NO_3^-).

Above results indicate that preparation methods and conditions largely affected nitrogen doping. N impurities (substitution for oxygen) are substitutionally doped into the TiO_2 lattice by annealing TiO_2 at high temperature under NH_3 flow, ion implantation and sputtering. However, nitrogen atom as an interstitial N impurity is bound to one or more lattice oxygen atoms by liquid-phase preparation at the lower temperatures [28,38] or microwave method. It also gives an explanation why the N peak at around 396 eV is not always observed for N-doped TiO_2 [31,38]. From the XPS spectra, we estimated that a nitrogen content of 3.7% (molar ratio) was incorporated into the TiO_2 prepared by the microwave method (N-TiO_2-M). In comparison, a lower nitrogen content of 2.2% (molar ratio) was detected in N-TiO_2-NH_3. The interstitial nitrogen seems to be more receptive for nitrogen-doped, whereas, the substitutional nitrogen doped into the TiO_2 lattice is not accessible because the bond of N–Ti is more difficult to form.

The Ti 2*p* XPS spectra for TiO_2–P25 and nitrogen-doped TiO_2 samples are shown in Fig.3(a). For TiO_2–P25, Ti $2p_{3/2}$ and $2p_{1/2}$ core level peaks appear at 458.9 and 464.7 eV, respectively, which are contributed by O–Ti–O in TiO_2 [10,28,29]. Compared with TiO_2–P25, the Ti 2*p* peaks for nitrogen-doped TiO_2 shift to the lower binding energies. These shifts of Ti $2p_{3/2}$ and $2p_{1/2}$ core level signal by 0.5–2 eV suggest the successful incorporation of nitrogen into the TiO_2 lattice [10,28]. In our research, we also found preparation methods and experimental conditions significantly affected the shift of the Ti 2*p* core levels. For N-TiO_2-NH_3, Ti $2p_{3/2}$ and $2p_{1/2}$ core level peaks appear at 457.9 and 463.5 eV, respectively, which are attributed to Ti 2*p* peaks of N–Ti–N or O–Ti–N in N-TiO_2 [28–30]. The BE of the Ti $2p_{3/2}$ peak shifts to the lowest energies by 1.0 and 1.2 eV compared with TiO_2–P25, when Ti^{4+} is reduced to Ti^{3+}. But for N-TiO_2-M, Ti $2p_{3/2}$ and $2p_{1/2}$ core level peaks appear at 458.2 and 464.0 eV, respectively, which only decrease by 0.7 eV compared with TiO_2–P25. This suggests that the TiO_2 lattice is considerably modified by

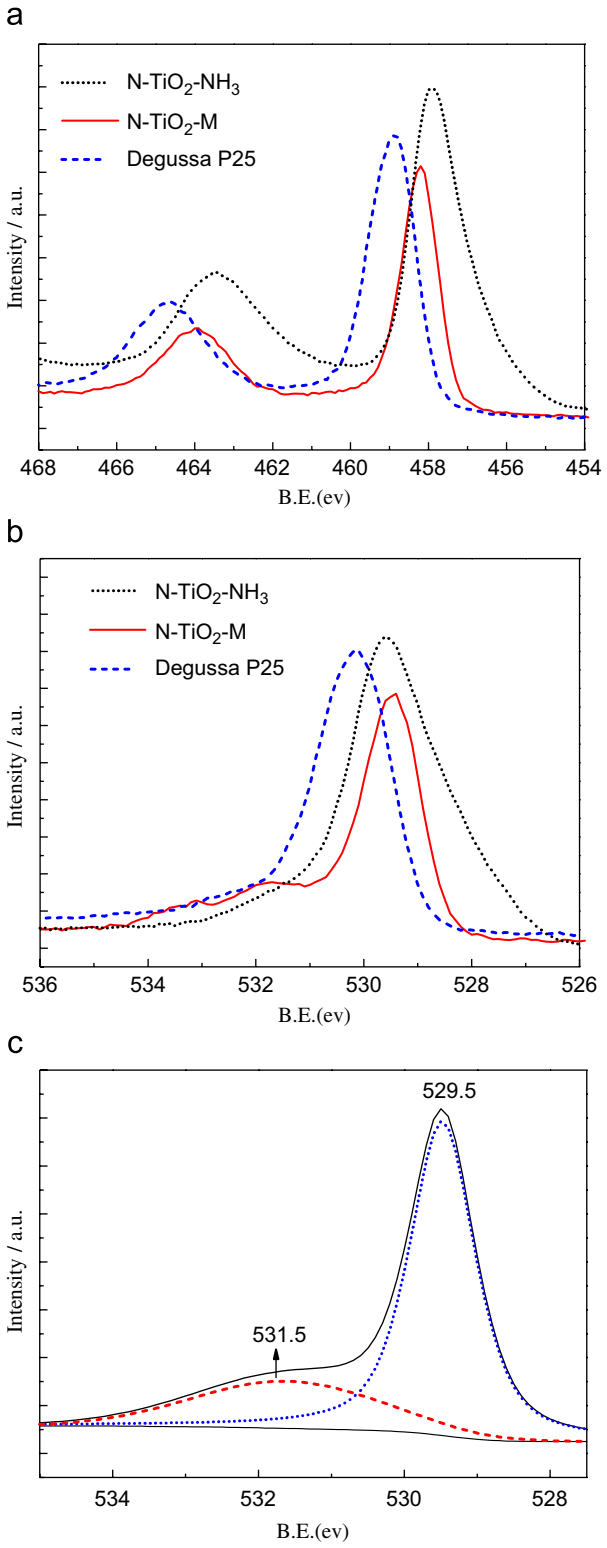

Fig. 3. XPS spectra of TiO_2 and N-TiO_2: (a) Ti 2*p*, (b) O 1*s* and (c) O 1*s* for N-TiO_2-M.

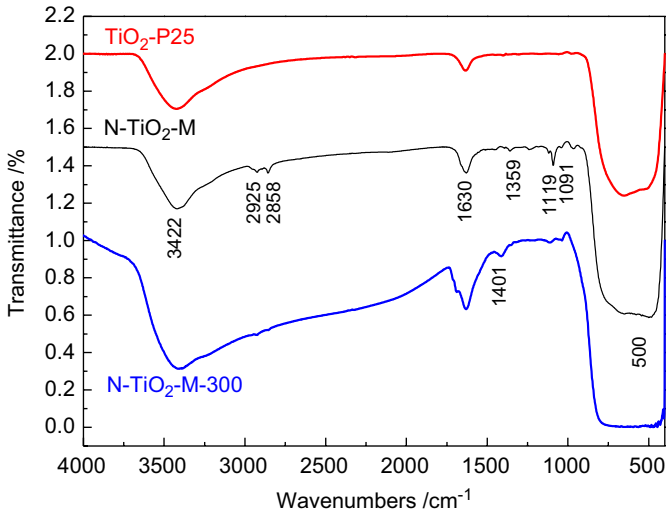

Fig. 4. FTIR spectra of P25, N-TiO_2-M and N-TiO_2-M-300.

interstitial-N for N-TiO_2-M in our experiment, which is not consistent with substitutional-N for N-TiO_2-NH_3.

In Fig. 3(b), the P25 sample shows an O 1*s* peak at 530.3 eV, which shifts to around 529.5 eV in N-TiO_2-M and N-TiO_2-NH_3. It is found that O 1*s* peak of nitrogen-doped TiO_2 shifts toward the lower binding energy, which is consistent with that of most reported [10,28,29]. An additional signal at higher binding energy (531.5 eV) was detected in N-TiO_2-M, as shown in Fig. 3(c). In view of O 1*s* peak of $-NO$ and $-NO_2$ on P25 at 533.5 eV [39], we suggest that the appearance of this peak at 531.5 eV is attributed to the formation of hyponitrite ($(N_2O_2)^{2-}$), due to the N interstitially doping into the TiO_2 lattice. It is further supported by N 1*s* XPS and FTIR analysis.

In the FTIR spectra in Fig. 4, two peaks at 3422 and 1630 cm^{-1} are assigned to the adsorbed water and hydroxyl on the surface of TiO_2. In the low frequency region of the spectra, fluctuant bands develop around 500 cm^{-1} are attributed to the anatase phase of TiO_2. Peaks at 2925, 2858 and 1359 cm^{-1} come from C–H ($\upsilon_{CH2,CH3}$ and $\delta_{CH2,CH3}$) of organic compound remained on N-TiO_2-M. After heat treatment at 300 °C, these peaks disappear in N-TiO_2-M-300. Compared with P25–TiO_2, new peaks around 1110 cm^{-1} appear in N-TiO_2-M. They are attributed to the formation of hyponitrite ($(N_2O_2)^{2-}$) [30,40], as demonstrated by XPS analysis. We did not find any peak assigned to N–H of NH_3 or urea adsorbed on the surface in the FTIR spectrum of N-TiO_2-M, suggesting that the hyponitrite is the characteristic structure of interstitial N for N-TiO_2-M prepared by microwave method.

The diffuse reflectance spectra of TiO_2–P25, N-TiO_2-M and N-TiO_2-NH_3 are shown in Fig. 5. Only a strong absorption that could be assigned to the band–band transition is observed in the ultraviolet region for pure P25–TiO_2. Compared with pure TiO_2, both N-TiO_2-M and N-TiO_2-NH_3 present a significant absorption in the visible region between 400 and 600 nm, which is the typical absorption feature of nitrogen-doped TiO_2. The light absorption of the N-TiO_2 in the visible light region is of great importance to its practical application since it can be activated even by solar light.

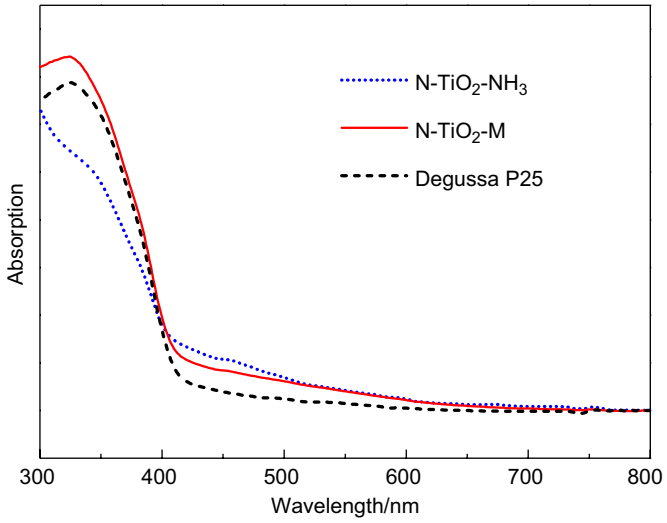

Fig. 5. UV–vis spectra of P25, N-TiO_2-M and N-TiO_2-NH_3.

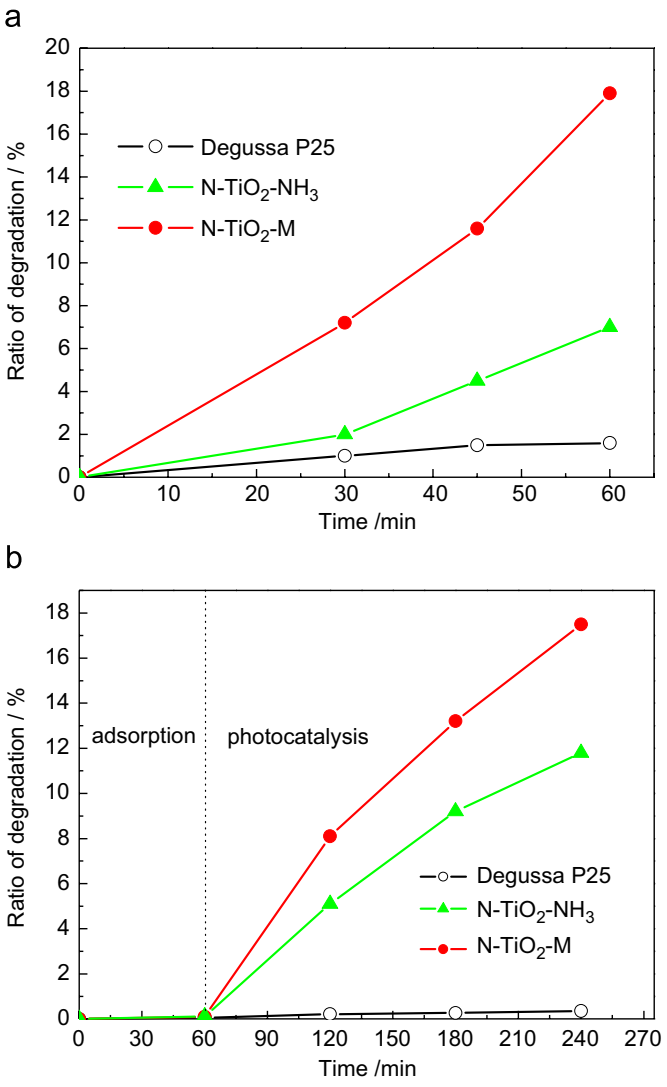

Fig. 6. Comparison of the photocatalytic decomposition of methyl orange (a) and phenol (b) under visible light irradiation on P25, N-TiO_2-M and N-TiO_2-NH_3. MO initial concentration of 20 mg/l and catalyst concentration of 0.1 g/l; phenol initial concentration of 100 mg/l and catalyst concentration of 0.2 g/l.

The photocatalytic activities of the catalysts were evaluated using the photodegradation of MO and phenol as model pollutant under visible light irradiation, as shown in Fig. 6. Low photocatalytic activity was observed for P25–TiO_2 under visible light due to their wide band gap. N-TiO_2-M and N-TiO_2-NH_3 have higher photocatalytic activities under visible light ($\lambda > 400$ nm), indicating that visible light can generate photon-induced electrons and holes in N-doped TiO_2. However, the N-TiO_2-M prepared by microwave method has a significantly higher photocatalytic activity for MO and phenol degradation under visible light than N-TiO_2-NH_3. Fig. 7 shows the reusability of N-TiO_2-M (M1–M3) and N-TiO_2-NH_3 (N1–N3) for phenol photocatalytic decomposition under visible light irradiation. No obvious loss of activity was observed for three runs. Thus, the N-TiO_2 can be used as a recyclable photocatalyst.

Asahi et al. thought that the oxygen sites were substituted by nitrogen atoms and these nitrogen sites were responsible for the visible light sensitivity, which is due to the narrowing of the band gap by mixing the N 2*p* and O 2*p* states [8]. But Hashimoto et al. suggested that the isolated N 2*p* narrow band above the O 2*p* valence band was responsible for the visible light response in the nitrogen-doped TiO_2 [21]. Di Valentin et al. provided theoretical evidence that [36,41] in the case of substitutional N-doped anatase TiO_2, the visible light response arises from occupied N 2*p* localized states slightly above the valence band edge; whereas in the case of interstitial N-doped anatase TiO_2, the visible light response arises from occupied π^* character N–O localized states slightly above the valence band edge. The highest localized state for the interstitial species is 0.73 eV above the top of the valence band, while this value is 0.14 eV for the substitutional species [41]. We present an electronic band schematics of photocatalytic reaction in visible light for substitutional and interstitial N-doped anatase TiO_2, as shown in Fig. 8. Compared with pure TiO_2 (UV region, $E > 3.2$ eV), visible light ($E < 3.0$ eV) can excite electrons from these occupied high energy states to the conduction band (CB). Some researches [11,31] presented that the interstitial N impurities might behave as stronger hole trapping sites, reducing the direct oxidation ability of sample in the photocatalytic process. However, we find interstitial N impurities can enhance the photoactivity of TiO_2 in visible light; moreover, the visible light activity is higher than that of substitutional N-doped TiO_2. According to Fig. 8, interstitial nitrogen states lie higher in the gap, thus excitation from the occupied high energy states to the CB is more favored than that of substitutional N-doped TiO_2. Therefore, we think that the microwave synthesis presented in this paper is a promising and practical method for producing interstitial nitrogen-doped photocatalyst with higher visible light activity.

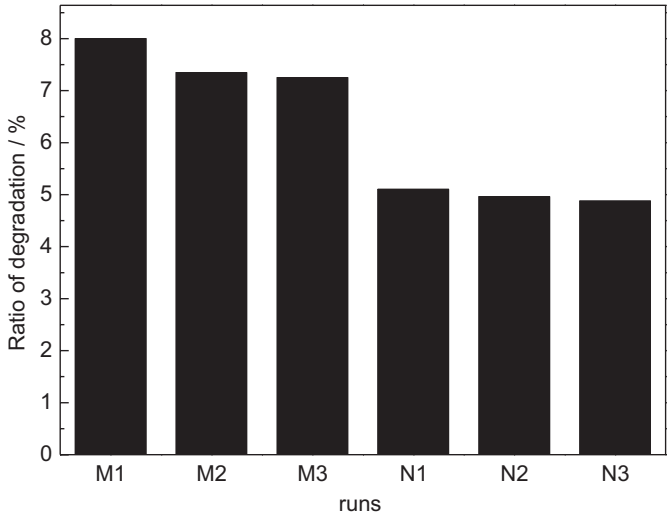

Fig. 7. Reusability of N-TiO_2-M (M1–M3) and N-TiO_2-NH_3 (N1–N3) for phenol photocatalytic decomposition under visible light irradiation. Phenol initial concentration of 100 mg/l; catalyst concentration of 0.2 g/l and reaction time of 1 h.

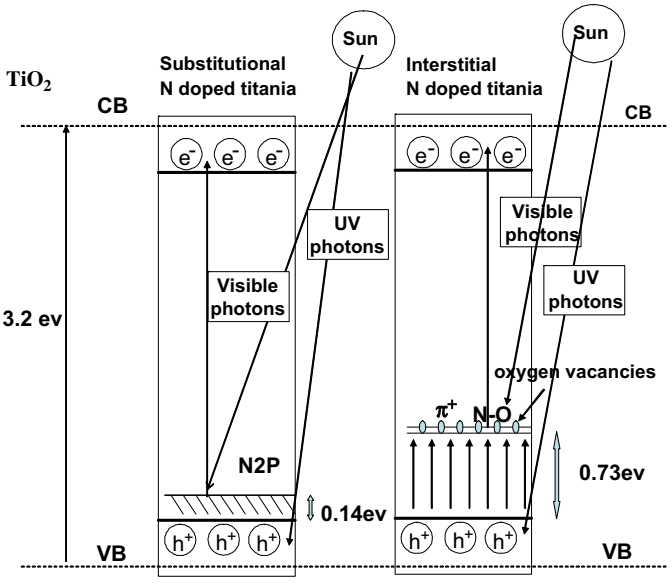

Fig. 8. Electronic band schematics of photocatalytic reaction for substitutional and interstitial N-TiO_2.

4. Conclusions

In conclusion, we prepared substitutional and interstitial N-doped TiO_2, which were used to decompose MO dye and phenol under visible radiation. The surface states of substitutional and interstitial N-doped TiO_2 were investigated based on XPS spectra of N 1*s*, O 1*s* and Ti 2*p*. The results indicate that the hyponitrite is the characteristic structure of interstitial N. Both substitutional and interstitial N impurities can enhance the photoactivity of TiO_2 in visible light. Moreover, the visible light activity of interstitial N-doped TiO_2 is higher than that of substitutional N-doped TiO_2. This study has also presented a promising and practical method for the production of interstitial nitrogen-doped photocatalyst.

Acknowledgments

The authors thank the Guangdong Provincial Natural Science Foundation of China (No. 05006553) and the Guangdong Provincial Science and Technology Project of China (No. 2005A10702002), for financial support.

References

[1] J.M. Wu, B. Qi, J. Phys. Chem. C 111 (2007) 666.
[2] O. Ozcan, F. Yukruk, E.U. Akkaya, D. Uner, Appl. Catal. B: Environ. 71 (2007) 291.
[3] D. Chatterjee, A. Mahata, Catal. Commun. 2 (2001) 1.
[4] S. Yin, K. Ihara, M. Komatsu, Q.W. Zhang, F. Saito, T. Kyotani, T. Sato, Solid State Commun. 137 (2006) 132.
[5] S.U.M. Khan, M. Al-Shahry, W.B. Ingler, Science 297 (2002) 2243.
[6] T. Umebayashi, T. Yamaki, S. Tanaka, K. Asai, Catal. Lett. 32 (2003) 330.
[7] J. Yang, H.Z. Bai, X.C. Tan, J.S. Lian, Appl. Surf. Sci. 253 (2006) 1988.
[8] R. Asahi, T. Morikawa, T. Ohwaki, K. Aoki, Y. Taga, Science 293 (2001) 269.
[9] C. Burda, Y.B. Luo, X.B. Chen, A.C.S. Samia, J. Stout, J.L. Gole, Nano. Lett. 3 (2003) 1049.
[10] M. Sathish, B. Viswanathan, R.P. Viswanath, C.S. Gopinath, Chem. Mater. 17 (2005) 6349.
[11] M. Mrowetz, W. Balcerski, A.J. Colussi, M.R. Hoffmann, J. Phys. Chem. B 108 (2004) 17269.
[12] Y. Liu, X. Chen, J. Li, C. Burda, Chemosphere 61 (2005) 11.
[13] X.H. Huang, Y.C. Tang, C. Hu, H.O. Yu, C.S. Chen, J. Environ. Sci. China 17 (2005) 562.
[14] T. Morikawa, R. Asahi, T. Ohwaki, A. Aoki, Y. Taga, Jpn. J. Appl. Phys. 40 (2001) 561.
[15] S. Sakthivel, H. Kisch, ChemPhysChem 4 (2003) 487.
[16] A. Ghicov, J.M. Macak, H. Tsuchiya, J. Kunze, V. Haeublein, S. Kleber, P. Schmuki, Chem. Phys. Lett. 419 (2006) 426.
[17] J. Premkumar, Chem. Mater. 16 (2004) 3980.
[18] S.M. Chiu, Z.S. Chen, K.Y. Yang, Y.L. Hsu, D. Gan, J. Mater. Process Tech. 192 (2007) 60.
[19] O. Diwald, T.L. Thompson, T. Zubkov, E.G. Goralski, S.D. Walck, J.T. Yates, J. Phys. Chem. B 108 (2004) 6004.
[20] T. Tachikawa, Y. Takai, S. Tojo, M. Fujitsuka, H. Irie, K. Hashimoto, T. Majima, J. Phys. Chem. B 110 (2006) 13158.
[21] H. Irie, Y. Watanabe, K. Hashimoto, J. Phys. Chem. B 107 (2003) 5483.
[22] Y. Guo, X.W. Zhang, W.H. Weng, G.R. Han, Thin Solid Films 515 (2007) 7117.
[23] N. Venkatachalam, A. Vinu, S. Anandan, B. Arabindoo, V. Murugesan, J. Nanosci. Nanotechnol. 6 (2006) 2499.
[24] T. Sano, N. Negishi, K. Koike, K. Takeuchi, S. Matsuzawa, J. Mater. Chem. 14 (2004) 380.
[25] H. Kisch, S. Sakthivel, M. Janczarekm, D. Mitoraj, J. Phys. Chem. C 111 (2007) 11445.
[26] I.C. Kang, Q.W. Zhang, J. Kano, S. Yin, T. Sato, F. Saito, J. Photochem. Photobiol. A: Chem. 189 (2007) 23297.
[27] M. Sathish, B. Viswanathan, R.P. Viswanath, C.S. Gopinath, Chem. Mater. 17 (2005) 6349.
[28] X.B. Chen, C. Burda, J. Phys. Chem. B 108 (2004) 15446.
[29] M.S. Wong, H.P. Chou, T.S. Yang, Thin Solid Films 494 (2006) 244.
[30] S. Sakthivel, M. Janczarek, H. Kisch, J. Phys. Chem. B 108 (2004) 19384.
[31] R. Nakamura, T. Tanaka, Y. Nakatio, J. Phys. Chem. B 108 (2004) 10617.

[32] P. Chen, W. Li, T.L. Zhou, Y.P. Jin, M.Y. Gu, J. Photochem. Photobiol. A: Chem. 168 (2004) 97.
[33] F. Peng, H.J. Wang, H. Yu, S.H. Chen, Mater. Res. Bull. 41 (2006) 2123.
[34] H.X. Li, J.X. Li, Y.I. Huo, J. Phys. Chem. B 110 (2006) 1559.
[35] N.C. Saha, H.G. Tompkins, J. Appl. Phys. 72 (1992) 3072.
[36] C. Di Valentin, G. Pacchioni, A. Selloni, S. Livraghi, E. Giamello, J. Phys. Chem. B 109 (2005) 11414.
[37] S. Livraghi, M.C. Paganini, E. Giamello, A. Selloni, C. Di Valentin, G. Pacchioni, J. Am. Chem. Soc. 128 (2006) 15666.
[38] S. Sakthivel, H. Kisch, Chem. Phys. Chem. 4 (2003) 487.
[39] J.A. Rodriguez, T. Jirsak, J. Dvorak, S. Sambasivan, D. Fischer, J. Phys. Chem. B 104 (2000) 319.
[40] J.A. Navio, C.C. Cerrillos, C. Real, Surf. Interface Anal. 24 (1996) 355.
[41] C. Di Valentin, G. Pacchioni, A. Selloni, Phys. Rev. B 70 (2004) 85116.